

**Molecular simulation of shocked materials using the reactive Monte Carlo method**

John K. Brennan and Betsy M. Rice

*Weapons and Materials Research Directorate, U.S. Army Research Laboratory, Aberdeen Proving Ground, Maryland 21005-5066*

(Received 8 April 2002; published 14 August 2002)

We demonstrate the applicability of the reactive Monte Carlo (RxMC) simulation method [J. K. Johnson, A. Z. Panagiotopoulos, and K. E. Gubbins, *Mol. Phys.* **81**, 717 (1994); W. R. Smith and B. Tříska, *J. Chem. Phys.* **100**, 3019 (1994)] for calculating the shock Hugoniot properties of a material. The method does not require interaction potentials that simulate bond breaking or bond formation; it requires only the intermolecular potentials and the ideal-gas partition functions for the reactive species that are present. By performing Monte Carlo sampling of forward and reverse reaction steps, the RxMC method provides information on the chemical equilibria states of the shocked material, including the density of the reactive mixture and the mole fractions of the reactive species. We illustrate the methodology for two simple systems (shocked liquid NO and shocked liquid N<sub>2</sub>), where we find excellent agreement with experimental measurements. The results show that the RxMC methodology provides an important simulation tool capable of testing models used in current detonation theory predictions. Further applications and extensions of the reactive Monte Carlo method are discussed.

DOI: 10.1103/PhysRevE.66.021105

PACS number(s): 82.60.-s, 82.40.Fp, 02.70.Tt, 47.40.-x

**I. INTRODUCTION**

The behavior of materials under conditions of extreme temperature and pressure is of critical importance in many fields of physics and fluid science [1–3]. The properties of materials at these conditions can be measured through shock experiments, which are capable of producing pressures up to several hundred gigapascal and temperatures exceeding 10 000 K. Moreover, determining the shock properties of energetic materials is a crucial task in the field of detonation science [4].

Experimental measurements of the properties of shocked materials are often difficult because instrumentation must be capable of spanning a wide range of pressures (1–300 GPa) and temperatures (500–15 000 K). Additionally, energy releases that might accompany a material under shock conditions, as well as the time and length scales over which the event occurs, have thwarted extensive experimental studies of many fundamental substances. As a further complication, recent theoretical predictions suggest that the detonation products of some systems supercritical phase separate, significantly altering the shock properties (see, e.g., Refs. [5–7]). Unfortunately, current experimental techniques are not capable of delineating the phase separation of materials under shock conditions, thus this behavior has not yet been verified.

Such laboratory challenges have necessitated the development of theoretical predictive capabilities to complement the experimental analyses. To date, the most reliable theoretical treatments for predicting shock properties apply statistical mechanical approaches such as variational perturbation theory (e.g., Ref. [8]) or integral equation theory (e.g., Refs. [9–11]). These approaches predict the shock properties by minimizing the Gibbs free energy and by requiring that the total number of elements constituting the chemically reacting species is conserved. Thermochemical software, such as the CHEMICAL EQUILIBRIUM (CHEQ) code [12] and CHEETAH [13] are capable of performing such calculations. However, these approaches require accurate equations of state (EOS) for the

reactive mixture, thus limiting the prediction of the shock properties of materials to those for which equations of state are available. The calculations also require heats of formation and densities of the unshocked material. These quantities are often unknown for notional or novel energetic materials, as well as for materials in highly nonideal environments (e.g., energetic materials packed in polymer matrices or confined in carbon nanotubes). Furthermore, approximations often must be made within the theoretical models to keep the calculations tractable, for example, to develop an analytical representation of the fluid equation of state [11] or in applying the van der Waals one-fluid approximation [12,13]. These types of approximations can add uncertainty to the predictive capabilities of the methods.

A powerful simulation method available for studying the shock properties of materials while providing insight into atomic-level phenomena is the molecular dynamics method (MD) [14–31]. The method can be used irrespective of rate limitations, the production of huge energy releases, extreme thermodynamic conditions, or other regimes that are presently inaccessible by experimental methods. MD evaluation of the Hugoniot states of a material can be accomplished by calculating properties behind the shock discontinuity in a shockwave simulation [30] or by generating an equation of state for subsequent evaluation of the Hugoniot conservation relations [24,27]. Recently, an equilibrium molecular dynamics method has been introduced, termed uniaxial Hugonostat [29], which utilizes equations of motion that constrain the system during the MD simulation such that the time-averaged properties correspond to those on the shock Hugoniot curve. For evaluating the shock Hugoniot of a material, the uniaxial Hugonostat technique is more efficient than the method of generating an EOS using standard molecular dynamics for subsequent evaluation of the conservation equations [24,27]. A significant drawback of all MD approaches, however, is that they require an accurate model of the interaction potential experienced between all species in the shocked and unshocked states. If the relative species concentrations of the products in the shocked state of interest are

not known, then the molecular dynamics approach requires an interaction potential that simulates bond breaking and bond formation in order to establish the chemical equilibrium of the final shocked state. Although significant advances have been made in developing potentials that reproduce the characteristics of a detonation, the potentials are still highly idealized representations of the energetic molecular system [14–23,25–28]. However, if the relative species concentrations are known at the conditions of the shocked state, then generating the shock Hugoniot curve using either the conventional or the uniaxial Hugoniot MD method only requires appropriate potentials that describe nonreactive interactions among all species present.

One of the several alternative methods for calculating chemically reactive systems (see Ref. [37] for a comprehensive review) which is appropriate for determining the shock properties of materials is the reactive Monte Carlo (RxMC) method [32,33]. The RxMC method circumvents some of the problems associated with conventional and uniaxial Hugoniot MD methods. The RxMC method requires neither *a priori* knowledge of the relative concentrations of the species in the shocked state nor a potential that describes bond breaking or bond formation. The method only requires: (a) functions that accurately describe nonreactive interactions between all possible species in the equilibrium mixture of the final shocked state (i.e., intermolecular potentials); and (b) ideal-gas partition functions for all species in the mixture. For a given intermolecular potential model, the method will provide information on the chemical equilibrium state, such as the density of the reactive mixture, the mole fractions of reactive species, the change in the total number of moles, and the internal energy. The intermolecular model can contain various levels of detail including multisite molecules and electrostatic contributions. Numerous reactions can be simulated simultaneously in multiple phase systems by performing Monte Carlo sampling of forward and reverse reaction steps. Using the reactive Monte Carlo method, the dependence of the chemical equilibria on system conditions such as temperature, pressure, and the surrounding environment (e.g., a condensed phase or highly nonideal environment) can be studied.

In this work we demonstrate the applicability of the reactive Monte Carlo method for calculating the shock Hugoniot properties of materials. We illustrate the method for two systems that have been studied extensively by both experimental and theoretical techniques. We consider shocked liquid NO, which is (nearly) an irreversible decomposition reaction that generates a mixture of homonuclear products ( $N_2$  and  $O_2$ ). We also consider shocked liquid  $N_2$ , which dissociates into atomic nitrogen (N) within a particular thermodynamic regime.

The outline of the paper is as follows. The reactive Monte Carlo methodology applied to the simulation of the shock properties of materials is described in Sec. II. Simulation details and models can be found in Sec. III, and application of the method to shocked liquid  $N_2$  and shocked liquid NO is presented in Sec. IV. Finally, discussion of the results and possible extensions of the method are given in Sec. V.

## II. METHODOLOGY

### A. Reactive Monte Carlo method

The RxMC method [32,33] is designed to minimize the Gibbs free energy, thus determining the true chemical equilibrium state irrespective of rate limitations. The RxMC method requires intermolecular potentials for the molecular species that are present in the reactive mixture, and often uses spherically averaged potentials such as Lennard-Jones or exponential-6 models [34]. The RxMC method also requires inputting the ideal-gas internal modes (vibration, rotation, electronic) for each reactive species. These contributions can be included by calculating internal partition functions from molecular energy-level data [32] or by using tabulated thermochemical data [33]. Regardless of the approach taken, the required information is readily available in standard sources [34–36] or can be generated using quantum mechanical calculations. Finally, the particular reactions occurring in the system must be specified. Provided that a sufficient set of independent reactions are specified, this requirement is not a considerably limiting factor since insignificant reactions are easily discernable by negligible product concentrations.

Implementation of the RxMC method provides information on the chemical equilibrium state, such as the density of the reactive mixture, mole fractions of reactive species, the change in the total number of moles, and the internal energy. The RxMC method can be performed in many different types of ensembles, including canonical, isothermal isobaric, Gibbs [37], and other less common ensembles [38]. Furthermore, the RxMC method can be performed for multiple reactions and multiple phases [32,33,37,39–43,45]. The RxMC method does not simulate bond breaking or bond formation; these relatively rare events in the standard Metropolis Monte Carlo method [46] would result in considerable statistical uncertainty. Rather, the RxMC method directly samples forward and reverse reaction steps as Monte Carlo type moves according to the stoichiometry of the reactions being sampled.

The isothermal-isobaric version of the RxMC method containing  $J$  number of reactions involves the following trial moves: (1) a change in the position or orientation of a molecule, chosen at random; (2) a forward step for randomly chosen reaction  $j$ , in which reactant molecules are chosen at random and changed to product molecules; (3) a reverse step for randomly chosen reaction  $j$ , in which product molecules are chosen at random and changed to reactant molecules; and (4) a random change in the simulation box volume.

Step (1) ensures that thermal equilibrium is established for the user-specified temperature, steps (2) and (3) ensure that chemical equilibrium is established, while step (4) satisfies the requirement of mechanical equilibrium for the user-specified pressure. Note that the transition probabilities in steps (2) and (3) do not require specifying the values of the chemical potentials or chemical potential differences for any of the mixture components.

The acceptance probability of state  $k$  going to state  $l$  for a particle displacement or orientation step is given by

$$P_{kl}^{\text{dis}} = \min\{1, \exp(-\beta\Delta U_{kl})\}, \quad (1)$$

where  $\Delta U_{kl} = U_l - U_k$  is the change in the configurational energy and  $\beta = 1/k_B T$ ;  $k_B$  is the Boltzmann constant and  $T$  is the temperature.

The acceptance probability for a reaction step is given by

$$P_{j,kl}^{\text{rxn}} = \min\left\{1, \prod_{i=1}^{c_j} \frac{N_i!}{(N_i + \nu_{ji}\xi_j)!} \left(\frac{q_{\text{int},i} V}{\Lambda_i^3}\right)^{\nu_{ji}\xi_j} \times \exp(-\beta\Delta U_{kl})\right\}, \quad (2)$$

where  $c_j$  is the total number of species in reaction  $j$ ;  $N_i$  is the total number of molecules of species  $i$ ;  $\nu_{ji}$  is the stoichiometric coefficient of species  $i$  in reaction  $j$ ;  $\xi_j$  is the molecular extent of reaction for reaction  $j$ ;  $q_{\text{int},i}$  is the quantum partition function for the internal modes of an isolated molecule of species  $i$ , which includes vibrational, rotational, and electronic modes;  $\Lambda_i$  is the thermal de Broglie wavelength of species  $i$ ; and  $V$  is the total volume of the system. Equation (2) is appropriate for both forward and reverse reaction steps ( $\xi_j = 1$  for a forward step and  $\xi_j = -1$  for a reverse step), where the stoichiometric coefficients are taken to be positive for product species and negative for reactant species. (For example, consider the reaction  $A \rightleftharpoons 2B$ . For the reaction as written, the stoichiometric coefficients for species  $A$  and  $B$  are  $\nu_A = -1$  and  $\nu_B = +2$  while  $\xi = +1$ . Then for the reverse reaction step,  $\nu_A$  and  $\nu_B$  again are  $-1$  and  $+2$ , respectively, but now  $\xi = -1$ .)

Finally, a random change in the simulation box volume is accepted with the probability

$$P_{kl}^{\text{vol}} = \min\left\{1, \exp\left(-\beta\Delta U_{kl} - \beta P_{\text{imp}}(V_l - V_k) + N \ln \frac{V_l}{V_k}\right)\right\}, \quad (3)$$

where  $P_{\text{imp}}$  is the user specified or *imposed* pressure. Derivations of these transition probabilities along with further details of the methodology can be found in the original papers [32,33,37].

### B. Calculation of shock Hugoniot properties

The thermodynamic quantities of a material in the initial unshocked state and the final shocked state are related by the conservation equations of mass, momentum, and energy across the shock front as [4]

$$\text{mass, } \rho_o D = \rho(D - u), \quad (4)$$

$$\text{momentum, } P - P_o = \rho_o u D, \quad (5)$$

$$\text{energy, } E - E_o = \frac{1}{2}(P + P_o)(V_o - V). \quad (6)$$

In Eqs. (4)–(6),  $E$  is the specific internal energy,  $P$  is the pressure,  $\rho$  is the specific density,  $V = 1/\rho$  is the specific volume,  $D$  is the velocity of the shock wave propagating through the material, and  $u$  is the mass velocity of the products behind the shock wave. The term *specific* refers to the

quantity per unit mass, while the subscript “ $o$ ” refers to the quantity in the initial unshocked state.

The shock wave velocity  $D$  can be calculated by solving Eqs. (4) and (5) for the mass velocity  $u$  and equating these expressions. The resulting expression, termed the Rayleigh line, can be written as

$$R = \rho_o^2 D^2 - (P - P_o)(V_o - V) = 0. \quad (7)$$

The so-called *Hugoniot* function satisfies Eq. (6) as

$$H_g(T, V) = 0 = E - E_o - \frac{1}{2}(P + P_o)(V_o - V). \quad (8)$$

Note that the quantities  $E$  and  $V$  are extensive quantities in Eqs. (6)–(8) and thus dependent on the relative amounts of the reactive species. The extensive quantities used in this work were formulated on a specific basis (per gram), alternatively these quantities can be formulated on a total system basis (total number of moles). The relative amounts of the reactive species along with the quantities  $E$ ,  $P$ , and  $V$  are calculated explicitly during the RxMC simulation. The internal energy is calculated during the RxMC simulation based upon the following derivation. The thermodynamic definition of the internal energy is given as

$$E \equiv H - PV, \quad (9)$$

where  $H$  is the specific enthalpy that can be written as a sum of the ideal gas ( $H^0$ ) and excess enthalpies ( $H^e$ ),

$$H = H^0 + H^e. \quad (10)$$

The ideal gas and excess enthalpies can be written as

$$H^0 = \sum_{i=1}^{c_j} y_i H_i^0 \quad (11)$$

and

$$H^e = U^{\text{conf}} + PV - RT, \quad (12)$$

so that

$$H = \sum_{i=1}^{c_j} y_i H_i^0 + U^{\text{conf}} + PV - RT. \quad (13)$$

$U^{\text{conf}}$  is the total configurational energy calculated during the simulation from the species-species interactions;  $y_i$  is the mole fraction of species  $i$ ;  $c_j$  is the total number of species;  $H_i^0$  is the specific ideal-gas enthalpy of pure species  $i$ , which can be determined solely from tabulated thermochemical data at the appropriate temperature  $T$  [36,47,48] or with tabulated thermochemical data supplemented with computed values where data are lacking (see, e.g., Refs. [49], [50]); and  $R$  is the universal gas constant. Then, substituting Eq. (13) into Eq. (9),

$$E = \sum_{i=1}^{c_j} y_i H_i^0 + U^{\text{conf}} - RT, \quad (14)$$

TABLE I. Exponential-6 potential parameters.

| Species        | $r_{\text{core}}$ (Å) | $r_m$ (Å) | $\varepsilon/k_B$ (K) | $\alpha$ | Source    |
|----------------|-----------------------|-----------|-----------------------|----------|-----------|
| N <sub>2</sub> | 1.13                  | 4.2005    | 101.10                | 12.684   | Ref. [11] |
| N              | 0.98                  | 2.5688    | 88.181                | 11.013   | Ref. [11] |
| NO             | 1.00                  | 3.995     | 117.1                 | 12.08    | Ref. [61] |
| N <sub>2</sub> | 0.98                  | 4.251     | 75.0                  | 13.474   | Ref. [61] |
| O <sub>2</sub> | 0.96                  | 4.110     | 75.0                  | 13.117   | Ref. [61] |

which is the specific internal energy expression needed in Eq. (8).

The search algorithm for locating a point on the Hugoniot curve used in this study is as follows.

(i) For a user-specified pressure  $P$  a few RxMC- $NPT$  simulations were performed at temperatures believed to be near  $H_g(T, V) = 0$ .

(ii) A functional form for the  $H_g$  vs  $T$  plot is determined, e.g., fitted to a quadratic polynomial, and the temperature ( $T_{H_g}$ ) that satisfies Eq. (8) at  $H_g = 0$  is interpolated.

(iii) Similarly, functional forms for the other desired quantities ( $V, E, D$ ) were determined and interpolated at  $T_{H_g}$ .

Depending on the initial guess of  $T_{H_g}$ , additional RxMC simulations may be required to achieve the desired accuracy. Typically, four to six RxMC simulations are needed to determine a single point on the Hugoniot curve, where best results are obtained when chosen values of  $T$  include both  $H_g > 0$  and  $H_g < 0$ . Steps (i) through (iii) are then repeated to trace out the entire Hugoniot curve.

### III. SIMULATION MODEL AND DETAILS

#### A. Intermolecular potential models

The species particles interact through the exponential-6 potential, which can be expressed as

$$U_{\text{exp-6}}(r) = \begin{cases} \infty, & r < r_{\text{core}} \\ \frac{\varepsilon}{1-6/\alpha} \left\{ \frac{6}{\alpha} \exp\left(\alpha \left[1 - \frac{r}{r_m}\right]\right) - \left(\frac{r_m}{r}\right)^6 \right\}, & r \geq r_{\text{core}}, \end{cases} \quad (15)$$

where  $\varepsilon$  is the depth of the attractive well between particles,  $r_m$  is the radial distance at which the potential is a minimum, while  $\alpha$  controls the steepness of the repulsive interaction. The cutoff distance  $r_{\text{core}}$  is included to avoid the unphysical singularity in the potential function as  $r \rightarrow 0$ . The potential parameters for the species considered in this work are given in Table I (first two entries: N<sub>2</sub> dissociation reaction; last three entries: NO decomposition reaction). A spherical cutoff for the particle-particle interactions was applied at  $4.5r_{m,\text{NO}}$  for the NO decomposition reaction without applying any correction for this truncation, while a spherical cutoff of  $2.5r_{m,\text{N}_2}$  was applied for the N<sub>2</sub> dissociation reaction with long range corrections added to account for interactions beyond this distance [51]. Electrostatic contributions were ig-

nored between species. The unlike interactions between species  $i$  and  $j$  were approximated by the Lorentz-Berthelot mixing rules [34] for  $\varepsilon_{ij}$ ,  $\alpha_{ij}$ , and  $r_{m,ij}$ ,

$$\varepsilon_{ij} = (\varepsilon_i \varepsilon_j)^{1/2}, \quad \alpha_{ij} = (\alpha_i \alpha_j)^{1/2},$$

$$r_{m,ij} = (r_{m,i} + r_{m,j})/2,$$

$$\text{while } r_{\text{core},ij} = (r_{\text{core},i} + r_{\text{core},j})/2. \quad (16)$$

The vibrational and rotational contributions to the ideal-gas partition functions used in simulating the NO decomposition reaction were calculated using a standard source [35] and supplemented with electronic level constants [36,52]. The vibrational and rotational contributions to the ideal-gas partition function of N<sub>2</sub> used in simulating the N<sub>2</sub> dissociation reaction were likewise calculated using a standard source [35] and supplemented with electronic level constants that included the ground state and six excited electronic states [47]. For N, the electronic energy levels were taken from Moore and Gallagher [48]. The corresponding thermochemical reference data were used in calculating the ideal-gas enthalpies ( $H_i^0$ ) required in Eq. (11) [36,47,48].

#### B. Simulation details

Constant-pressure RxMC simulations of shocked N<sub>2</sub> and shocked NO were initiated from 3375 particles of N<sub>2</sub> and NO, respectively, placed on a face-centered-cubic lattice structure. The standard periodic boundary conditions and minimum image convention were used [53]. Simulations were performed in steps, where a step (chosen with equal probability) was either a particle displacement, forward reaction, step, or reverse reaction step. A change in the simulation cell volume was attempted every 2500 steps. Simulations were equilibrated for  $0.3 \times 10^7$  steps after which averages of the quantities were taken over  $2.0 \times 10^7$  steps. Uncertainties were estimated using the method of block averages by dividing the production run into ten equal blocks [51]. Reported uncertainties are one standard deviation of the block averages. The maximum displacement and volume change were adjusted to achieve an acceptance fraction of approximately 0.33 and 0.5, respectively. Depending on the system conditions, the acceptance fraction of the reaction steps ranged from 0.075–0.375. Calculated quantities were reduced by the exponential-6 potential energy ( $\varepsilon$ ) and size ( $r_m$ ) parameters (N<sub>2</sub> dissociation reaction, N<sub>2</sub> parameters; NO decomposition reaction, NO parameters).

### IV. APPLICATION

#### A. Shock Hugoniot states of liquid N<sub>2</sub>

We consider shocked N<sub>2</sub> in the pressure range 3–90 GPa for which reliable experimental data are available [54,55]. At pressures between approximately 30–100 GPa, the N≡N triple bond is destabilized and molecular nitrogen dissociates into atomic nitrogen [56,57]. At higher pressures, theory suggests that nitrogen can exist as a metastable polymeric phase of N atom clusters that are covalently bonded [58–62], before losing this covalency at still higher pressures. In the

TABLE II. Initial fluid states used to evaluate Eq. (8).

| Thermodynamic property               | Liquid N <sub>2</sub> |                  | Liquid NO            |               |
|--------------------------------------|-----------------------|------------------|----------------------|---------------|
|                                      | Experiment [55]       | NVT-MC           | Experiment [61]      | NVT-MC        |
| Temperature, $T$ (K)                 | 77.0<br>±0.5          | 77.0             | 122.6<br>+2.3/-1.1   | 122.6         |
| Density, $\rho$ (g/cm <sup>3</sup> ) | 0.808<br>±0.003       | 0.808            | 1.263<br>+0.06/-0.11 | 1.265         |
| Pressure, $P$ (MPa)                  |                       | 50.49<br>±0.02   |                      | 490.5<br>±0.1 |
| Energy, $E$ (kJ/g)                   |                       | -0.441<br>±0.004 | 2.650<br>±0.01       | 2.60<br>±0.01 |

present work, we consider only the regime where molecular nitrogen is believed to dissociate into atomic nitrogen,  $N_2 \rightleftharpoons 2N$ . Analogous to the work of Fried and Howard [11], we consider two models for this reaction, a *reactive* model that includes the dissociation reaction, and a *nonreactive* model that does not.

We determined the shock Hugoniot properties of liquid N<sub>2</sub> using the calculated initial states given in Table II. The values given in Table II were determined by performing a canonical ensemble (constant-NVT) Monte Carlo simulation of  $N=3375$  N<sub>2</sub> molecules at  $T=77.0$  K and at a specific volume of  $V=1.238$  cm<sup>3</sup>/g. A comparison of the pressure and internal energy determined from this NVT simulation with experiment is given in Table II. The shock Hugoniot properties were determined by carrying out the prescription outlined in Sec. II B. The raw data determined from a series of constant-pressure RxMC simulations at several different temperatures are given in the Appendix (Table V). Also reported in Table V are the values of the Hugoniot expression [Eq. (8)] using the predicted thermodynamic data. Quadratic polynomials were used in the fitting procedure of steps (ii) and (iii) (see Sec. II B) with the exception of the shock wave velocity ( $D$ ) where a linear equation was used. A comparison of the shock properties along the principal Hugoniot calcu-

lated from the RxMC simulations and the available experimental data is given in Table III. In Table III, the uncertainties for the shock Hugoniot properties measured by experiment are given in parentheses, while the uncertainties in the RxMC calculations can be estimated from the  $R$ -square value of the functional fit of data given in the Appendix. Typical  $R$ -square values for the predicted temperatures and specific volumes are 0.97–0.99. Plots of the shock Hugoniot pressure versus the specific volume and the shock wave velocity are given in Figs. 1 and 2, respectively, for both the reactive and nonreactive models.

We found excellent agreement between the RxMC calculations using the reactive model and the experimental measurements for most of the pressures considered. As the pressure is increased along the Hugoniot, the system becomes a partially dissociated fluid containing a mixture of N<sub>2</sub> molecules and N atoms. This behavior is reflected in the species mole fractions plot of Fig. 3. Values of the mole fractions shown in Fig. 3 were determined by interpolating the data reported in Table V to  $T_{H_g}$  using a quadratic function. It is evident from Fig. 1 that the nonreactive model fails at high pressures where the dissociation is not negligible [11].

The experimental data appear to exhibit a softening of the Hugoniot curve near 55 GPa while the RxMC simulations do not predict this behavior. Experimental errors are increasing in this region, therefore whether the discrepancy is due to experimental uncertainty or an inaccurate model cannot be conclusively established [11]. Interestingly, however, recent density-functional theory (DFT) calculation [31] predict the softening behavior. Pair correlation calculations in the work of Kress *et al.* [31] indicate that the system contains a small fraction of clusters larger than dimers in the partially dissociated region, however, these larger clusters are not long lived. The dissociated system may contain N<sub>*n*</sub> molecules bound by single (N—N) or single and double (N=N) bonds. Although refining the N<sub>2</sub> model is beyond the scope of the present work, such products and their accompanying reactions could be included into the RxMC simulation scenario, e.g.,  $N \equiv N \rightleftharpoons N = N$  or  $N \equiv N \rightleftharpoons N - N$ , which may

TABLE III. Shock Hugoniot states of liquid nitrogen. RxMC results are for the *reactive* model discussed in the text. Experimental data are taken from Nellis *et al.* [55], except for those noted. Uncertainties in experimental data (where available) are given in parentheses.

| $P$ (GPa)         |                   | $v$ (cm <sup>3</sup> /mole N <sub>2</sub> ) |       | $T$ (K)       |          | $D$ (km/s) |        |
|-------------------|-------------------|---|-------|---------------|----------|------------|--------|
| Experiment        | RxMC <sup>a</sup> | Experiment                                  | RxMC  | Experiment    | RxMC     | Experiment | RxMC   |
| 2.96 <sup>b</sup> | 2.96              | 21.7  | 21.36 |               | 536.2    | 3.14       | 3.087  |
| 4.74 <sup>b</sup> | 4.74              | 20.1  | 19.82 |               | 883.9    | 3.74       | 3.703  |
| 10.1 <sup>b</sup> | 10.0              | 17.3  | 17.41 |               | 2008.4   | 5.00       | 4.993  |
| 18.1 (0.5)        | 18.1              | 15.34 (0.5)                                 | 15.57 | 4300 (200)    | 3912.4   | 6.34       | 6.384  |
| 29.9 (0.5)        | 29.9              | 14.26 (0.5)                                 | 14.05 | 7300 (250)    | 6778.1   | 7.93       | 7.895  |
| 36.0 (0.4)        | 36.0              | 13.41 (0.4)                                 | 13.35 | 8750 (300)    | 7963.0   | 8.52       | 8.519  |
| 47.0 (0.5)        | 47.0              | 11.83 (0.5)                                 | 12.20 | 8900 (600)    | 9557.7   | 9.40       | 9.483  |
| 52.6 (0.5)        | 52.6              | 11.13 (0.5)                                 | 11.66 | 11 100 (800)  | 10 185.4 | 9.79       | 9.914  |
| 60.4 (0.7)        | 60.4              | 10.31 (0.7)                                 | 10.97 | 12 000 (850)  | 10 935.2 | 10.31      | 10.465 |
| 81.1 (1.5)        | 81.1              | 9.40 (1.5)                                  | 9.366 | 14 500 (1000) | 12 588.9 | 11.73      | 11.724 |

<sup>a</sup>Pressure imposed in the constant-pressure version of the RxMC method.<sup>b</sup>Taken from Zubarev and Telegin [54].

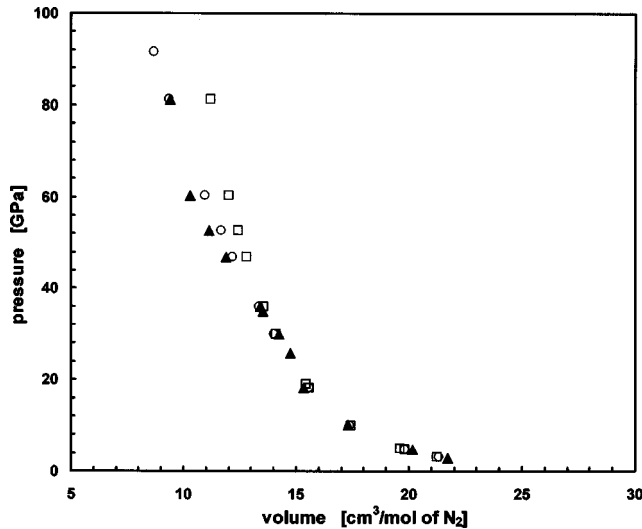


FIG. 1. The shock Hugoniot of liquid  $N_2$ . The values calculated from the RxMC simulations using a reactive ( $\circ$ ) and a nonreactive ( $\square$ ) model are compared with the experimental data ( $\blacktriangle$ ) [54,55]. The shock pressure is plotted vs the molar volume of  $N_2$ .

make RxMC calculations more compatible with the experimental measurements.

As a matter of curiosity, a point along the Hugoniot curve at  $P=91.5$  GPa was calculated. Although experimental data are not presently available at this pressure, the recent DFT calculations of Kress and co-workers [31] predict considerably different behavior in this pressure regime. The model used in the present work predicts softening behavior ( $v=8.68$   $\text{cm}^3/\text{mole } N_2$ ), as does the work of Fried and Howard [11], while the DFT calculations appear to be approaching a maximum compression in this region ( $v=9.34$   $\text{cm}^3/\text{mole } N_2$  at  $P=91.5$  GPa [31]). According to our calculations, such a system would contain a nearly

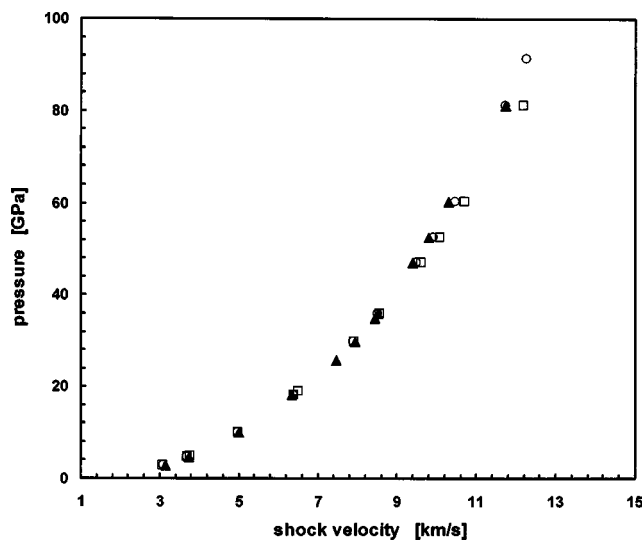


FIG. 2. The shock Hugoniot of liquid  $N_2$ . The values calculated from the RxMC simulations [reactive model ( $\circ$ ), nonreactive model ( $\square$ )] are compared with the experimental data ( $\blacktriangle$ ) [54,55]. The shock pressure is plotted vs the shock wave velocity.

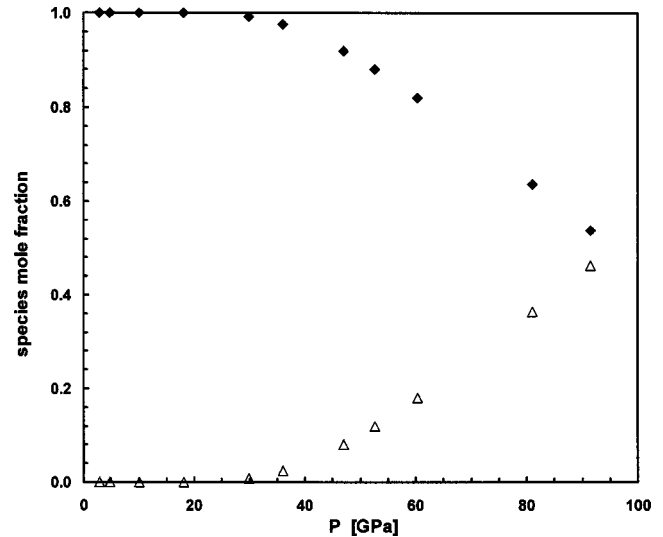


FIG. 3. Species mole fractions [ $N_2$  ( $\blacklozenge$ ), N ( $\triangle$ )] along the Hugoniot curve, determined from the RxMC simulations of the  $N_2$  dissociation reaction.

equimolar mixture of  $N_2$  molecules and dissociated N atoms (see Fig. 3).

### B. Shock Hugoniot states of liquid NO

Next, we consider the decomposition of nitric oxide:  $2NO \rightleftharpoons N_2 + O_2$ . This reaction generates a mixture of homonuclear products that are miscible with each other and (assumed to be) with residual NO. The concentrations of other products such as  $NO_2$  are considered to be negligible as are the accompanying reactions, e.g.,  $\frac{1}{2}N_2 + O_2 \rightleftharpoons NO_2$ .

We determined the shock Hugoniot properties of liquid NO using the calculated initial conditions given in Table II. An NVT Monte Carlo simulation was performed for  $N=3375$  NO molecules at  $T=122.6$  K and at a specific volume of  $V=0.7905$   $\text{cm}^3/\text{g}$ . The calculated pressure and internal energy from this simulation are compared with the experimental measurements in Table II. The shock Hugoniot properties were again determined by the prescription outlined in Sec. II B. The raw simulation data and the calculated quantities determined from a series of constant-pressure RxMC simulations at several different temperatures are given in the Appendix (Table VI). Quadratic polynomials were used in the fitting procedure (see Sec. II B) with the exception of the shock wave velocity ( $D$ ) where a linear equation was used. A comparison of the shock properties along the principal Hugoniot calculated from the RxMC simulations and the experimental data of Schott, Shaw, and Johnson [63] is given in Table IV. In Table IV, an estimate of the uncertainties in the RxMC calculations of the shock Hugoniot properties can be determined from the  $R$ -square value of the functional fit of data given in Appendix B. Typical  $R$ -square values for the predicted temperatures and specific volumes are 0.97–0.99. Plots of the shock Hugoniot pressure versus the specific volume and the shock wave velocity are given in Figs. 4 and 5, respectively. Again, excellent agreement between the RxMC calculations and the ex-

TABLE IV. Shock Hugoniot states of liquid nitric oxide. Experimental data are taken from Schott, Shaw, and Johnson [63].

| $P$ (GPa)  |                   | $V$ ( $\text{cm}^3/\text{g}$ ) |        | $T$ (K)    |      | $D$ (km/s) |       | $E$ (kJ/g) |       |
|------------|-------------------|--------------------------------|--------|------------|------|------------|-------|------------|-------|
| Experiment | RxMC <sup>a</sup> | Experiment                     | RxMC   | Experiment | RxMC | Experiment | RxMC  | Experiment | RxMC  |
| 14.47      | 14.47             | 0.5203                         | 0.5215 | 3064.9     |      | 5.767      | 5.700 | 4.663      | 4.611 |
| 17.93      | 17.93             | 0.483                          | 0.4868 | 3278.9     |      | 6.033      | 5.992 | 5.437      | 5.395 |
| 21.03      | 21.03             | 0.4627                         | 0.4622 | 3488.2     |      | 6.337      | 6.255 | 6.087      | 6.132 |
| 25.47      | 25.47             | 0.437                          | 0.4340 | 3819.1     |      | 6.715      | 6.619 | 7.157      | 7.227 |
| 28.47      | 28.47             | 0.4212                         | 0.4180 | 4074.4     |      | 6.940      | 6.853 | 7.903      | 7.993 |

<sup>a</sup>Pressure imposed in the constant-pressure version of the RxMC method.

perimental measurements is found with typical differences of 1–2%. Plots of the species mole fractions along the Hugoniot curve are shown in Fig. 6. Values of the mole fractions shown are interpolated from the data given in Table VI to  $T_{H_g}$  using a quadratic function. Since the mole fractions of  $\text{N}_2$  and  $\text{O}_2$  are equivalent, their mole fractions are plotted as “products” in Fig. 6. It is evident from Fig. 6 that as the pressure increases along the Hugoniot curve, the reaction equilibria shifts to an increasing amount of NO.

## V. DISCUSSION

We have demonstrated the effectiveness of using the reactive Monte Carlo simulation method for determining the shock properties of materials. We found the RxMC calculations to be in excellent agreement with the available experimental data for two simple systems. These demonstrations have illustrated the utility of the method for predicting the shock Hugoniot of mixtures for which species concentrations are not known and in the absence of interaction potentials that simulate bond breakage and formation.

Subsequent to the validation of the method presented in this paper, there are several possible extensions of the current

RxMC methodology. First, although the computations are reasonably inexpensive, it may be possible to reformulate the method within other ensembles (e.g., constant pressure, constant enthalpy, and constant number of particles [ $NPH$ ]), allowing the calculation of the Hugoniot curve to be carried out more efficiently and conveniently [38]. Further, the RxMC method has been recently combined with transition state theory to allow for the calculation of reaction rates [44]. Thus, extension of the method to reaction rate calculations for materials under shock may also be possible.

A coordinated approach that links experimental, theoretical, and RxMC efforts appears promising in furthering our understanding of chemical reacting systems in highly non-ideal environments. The RxMC method can perform several different functions in such approaches. First, the RxMC method can play a critical role in assessing theoretical models used in thermochemical codes such as CHEETAH [13] and CHEQ [12]. In these approaches, predictions using the model are usually obtained through approximate methods. Molecular simulation, on the other hand, provides an essentially exact result (within statistical uncertainty) for the model being considered and thus provides a means of testing these

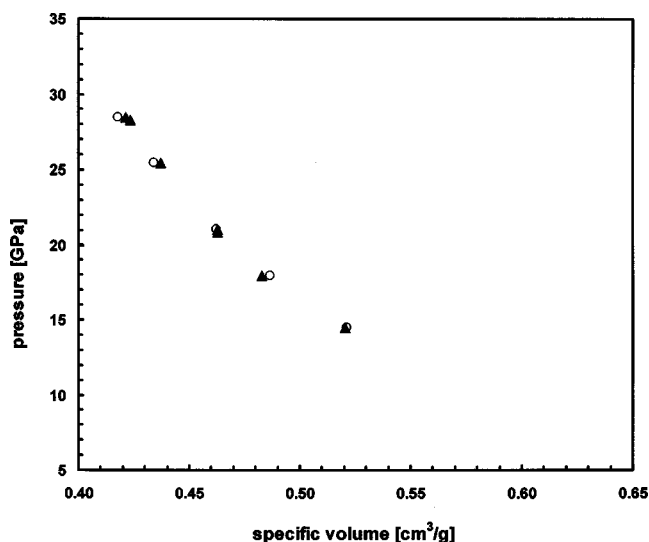


FIG. 4. The shock Hugoniot of liquid NO. The values calculated from the RxMC simulations ( $\circ$ ) model are compared with the experimental data ( $\blacktriangle$ ) [61]. The shock pressure is plotted vs the specific volume.

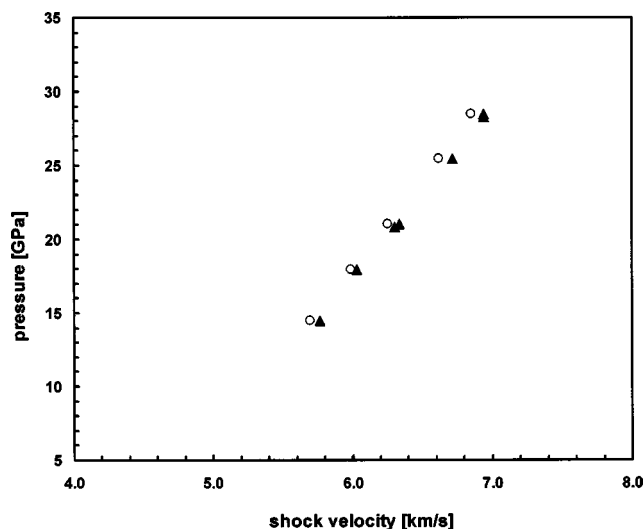


FIG. 5. The shock Hugoniot of liquid NO. The values calculated from the RxMC simulations ( $\circ$ ) model are compared with the experimental data ( $\blacktriangle$ ) [61]. The shock pressure is plotted vs the shock wave velocity.

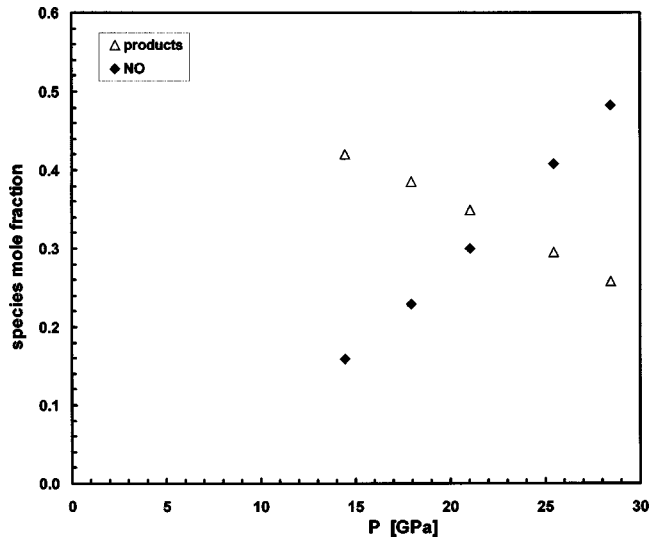


FIG. 6. Species mole fractions [NO ( $\blacklozenge$ ), either  $N_2$  or  $O_2$  ( $\triangle$ )] along the Hugoniot curve, determined from the RxMC simulations of the NO decomposition reaction. Mole fractions plotted as “products” represent the values for both  $N_2$  and  $O_2$ .

approximations. Furthermore, the underlying model of the theory can be tested by comparisons of simulation results to experiment.

The RxMC method can also be a powerful tool in the development of novel energetic materials. In lieu of the synthesis of a candidate material and the measurement of its thermophysical properties, quantum mechanical information can be generated to provide the ideal-gas partition functions

required for the simulation, while *ab initio* calculations can be used to parametrize the functions that describe the intermolecular interactions between the reactant and the species believed to exist in the product mixture. With these quantities in hand, the RxMC method can be used to predict shock properties of the notional material, thus providing crucial detonation performance information while avoiding costly and time-consuming experimental measurements.

The RxMC method can also be used to study the reactions of energetic materials in other nonideal environments, e.g., confined within polymer membranes, carbon nanotubes, or other porous materials, or for naval applications near or under water. Finally, the RxMC method can be applied to the study of the supercritical phase separation behavior that theory suggests occurs for some detonation products (see, e.g., Refs. [5–7]). Presently, this behavior has not been verified by experimental measurements. As noted in Sec. I, the RxMC method can be used to simulate multiple phase systems. Application of the method to such systems may provide further insight into this phenomenon.

#### ACKNOWLEDGMENTS

The authors wish to thank Martin Lisal (Institute of Chemical Process Fundamentals, Academy of Sciences of the Czech Republic) for helpful discussions and a critical reading of this manuscript prior to publication. J.K.B. thanks the National Research Council Associateship program and the U.S. Army Research Laboratory for support. The calculations reported in this work were performed at the Army Research Laboratory Major Shared Resource Center, Aberdeen Proving Ground, MD.

#### APPENDIX

TABLE V. Constant-pressure reactive Monte Carlo simulations of shocked liquid  $N_2$ . “ $\langle \rangle$ ” indicates ensemble averages determined from the simulation. Uncertainty in units of the last decimal digit is given in parentheses, 3.010(2) means  $3.010 \pm 0.002$ .

| T<br>(K)                    | $\langle P \rangle$<br>(GPa) | Mole fraction <sup>a</sup> |                        | $\langle V \rangle$<br>(cm <sup>3</sup> /g) | $\langle U^{\text{conf}} \rangle$<br>(kJ/g) | $H^{0b}$<br>(kJ/g) | $E^c$<br>(kJ/g) | $H_g^d$<br>(kJ/g) | $D^e$<br>(km/s) |
|-----------------------------|------------------------------|----------------------------|------------------------|---|---|--------------------|-----------------|-------------------|-----------------|
|                             |                              | $\langle x(N_2) \rangle$   | $\langle x(N) \rangle$ |   |   |                    |                 |                   |                 |
| $P_{\text{imp}} = 2.96$ GPa |                              |                            |                        |   |   |                    |                 |                   |                 |
| 475                         | 3.010(2)                     | 1.0000                     | 0.0000                 | 0.7532(8)                                   | 0.182(2)                                    | 0.1852             | 0.227           | -0.0732           | 3.059           |
| 500                         | 3.008(1)                     | 1.0000                     | 0.0000                 | 0.7572(7)                                   | 0.188(2)                                    | 0.2110             | 0.250           | -0.0429           | 3.071           |
| 525                         | 3.008(2)                     | 1.0000                     | 0.0000                 | 0.7606(9)                                   | 0.192(3)                                    | 0.2379             | 0.274           | -0.0138           | 3.082           |
| 550                         | 3.008(2)                     | 1.0000                     | 0.0000                 | 0.7646(9)                                   | 0.197(3)                                    | 0.2643             | 0.298           | 0.0165            | 3.094           |
| $P_{\text{imp}} = 4.74$ GPa |                              |                            |                        |   |   |                    |                 |                   |                 |
| 850                         | 4.795(3)                     | 1.0000                     | 0.0000                 | 0.7047(6)                                   | 0.463(4)                                    | 0.5955             | 0.806           | -0.0433           | 3.693           |
| 900                         | 4.795(3)                     | 0.9998(1)                  | 0.0002(1)              | 0.7090(8)                                   | 0.471(3)                                    | 0.6566             | 0.860           | 0.0210            | 3.708           |
| 950                         | 4.790(3)                     | 0.9997(1)                  | 0.0003(1)              | 0.7132(6)                                   | 0.478(5)                                    | 0.7201             | 0.916           | 0.0879            | 3.721           |
| $P_{\text{imp}} = 10.0$ GPa |                              |                            |                        |   |   |                    |                 |                   |                 |
| 1950                        | 10.072(7)                    | 1.0000                     | 0.0000                 | 0.6197(9)                                   | 1.249(7)                                    | 1.9407             | 2.611           | -0.0751           | 4.984           |
| 2000                        | 10.081(4)                    | 0.9998(1)                  | 0.0002(1)              | 0.6210(6)                                   | 1.254(9)                                    | 2.0101             | 2.670           | -0.0115           | 4.992           |
| 2050                        | 10.066(8)                    | 0.9998(1)                  | 0.0002(1)              | 0.6235(6)                                   | 1.260(9)                                    | 2.0749             | 2.726           | 0.0609            | 4.998           |
| $P_{\text{imp}} = 18.1$ GPa |                              |                            |                        |   |   |                    |                 |                   |                 |
| 3850                        | 18.195(2)                    | 0.9997(1)                  | 0.0003(1)              | 0.5549(7)                                   | 2.398(2)                                    | 4.4512             | 5.707           | -0.0806           | 6.380           |
| 3900                        | 18.191(2)                    | 0.9997(1)                  | 0.0003(1)              | 0.5557(7)                                   | 2.401(1)                                    | 4.5179             | 5.761           | -0.0168           | 6.383           |
| 3950                        | 18.189(2)                    | 0.9997(1)                  | 0.0003(1)              | 0.5569(8)                                   | 2.407(2)                                    | 4.5851             | 5.820           | 0.0533            | 6.388           |

TABLE V. (Continued).

| $T$<br>(K)                  | $\langle P \rangle$<br>(GPa) | Mole fraction <sup>a</sup> |                        | $\langle V \rangle$<br>(cm <sup>3</sup> /g) | $\langle U^{\text{conf}} \rangle$<br>(kJ/g) | $H^{\text{0b}}$<br>(kJ/g) | $E^{\text{c}}$<br>(kJ/g) | $H_g^{\text{d}}$<br>(kJ/g) | $D^{\text{e}}$<br>(km/s) |
|-----------------------------|------------------------------|----------------------------|------------------------|---|---|---------------------------|--------------------------|----------------------------|--------------------------|
|                             |                              | $\langle x(N_2) \rangle$   | $\langle x(N) \rangle$ |   |   |                           |                          |                            |                          |
| $P_{\text{imp}} = 29.9$ GPa |                              |                            |                        |   |   |                           |                          |                            |                          |
| 6700                        | 30.023(2)                    | 0.9930(1)                  | 0.0070(1)              | 0.5001(8)                                   | 3.963(1)                                    | 8.5267                    | 10.502                   | -0.1103                    | 7.890                    |
| 6725                        | 30.015(2)                    | 0.9939(1)                  | 0.0061(1)              | 0.5017(8)                                   | 3.960(2)                                    | 8.5392                    | 10.503                   | -0.0810                    | 7.897                    |
| 6750                        | 30.008(3)                    | 0.9936(1)                  | 0.0064(1)              | 0.5024(7)                                   | 3.966(3)                                    | 8.5808                    | 10.543                   | -0.0274                    | 7.900                    |
| 6775                        | 30.009(2)                    | 0.9926(1)                  | 0.0075(1)              | 0.5008(7)                                   | 3.954(2)                                    | 8.6431                    | 10.586                   | -0.0089                    | 7.892                    |
| 6800                        | 30.002(2)                    | 0.9923(1)                  | 0.0077(1)              | 0.5010(7)                                   | 3.957(1)                                    | 8.6847                    | 10.624                   | 0.0271                     | 7.895                    |
| $P_{\text{imp}} = 36.0$ GPa |                              |                            |                        |   |   |                           |                          |                            |                          |
| 7900                        | 36.083(3)                    | 0.9762(1)                  | 0.0238(1)              | 0.4762(9)                                   | 4.666(2)                                    | 10.8830                   | 13.204                   | -0.1105                    | 8.514                    |
| 7950                        | 36.121(3)                    | 0.9753(1)                  | 0.0247(1)              | 0.4765(6)                                   | 4.672(2)                                    | 10.9868                   | 13.299                   | -0.0252                    | 8.520                    |
| 7975                        | 36.100(2)                    | 0.9750(1)                  | 0.0250(1)              | 0.4766(5)                                   | 4.668(2)                                    | 11.0363                   | 13.338                   | 0.0233                     | 8.518                    |
| 8000                        | 36.143(2)                    | 0.9744(1)                  | 0.0256(1)              | 0.4766(5)                                   | 4.677(2)                                    | 11.0924                   | 13.395                   | 0.0644                     | 8.523                    |
| 8050                        | 36.141(2)                    | 0.9734(1)                  | 0.0266(1)              | 0.4768(7)                                   | 4.675(2)                                    | 11.2008                   | 13.486                   | 0.1606                     | 8.524                    |
| 8475                        | 36.120(3)                    | 0.9648(1)                  | 0.0352(1)              | 0.4796(11)                                  | 4.686(2)                                    | 12.1361                   | 14.307                   | 1.0393                     | 8.537                    |
| 8500                        | 36.115(3)                    | 0.9643(1)                  | 0.0357(1)              | 0.4796(5)                                   | 4.682(2)                                    | 12.1932                   | 14.352                   | 1.0863                     | 8.536                    |
| 8550                        | 36.119(3)                    | 0.9632(1)                  | 0.0368(1)              | 0.4800(8)                                   | 4.687(2)                                    | 12.3059                   | 14.455                   | 1.1950                     | 8.539                    |
| $P_{\text{imp}} = 47.0$ GPa |                              |                            |                        |   |   |                           |                          |                            |                          |
| 9350                        | 47.152(5)                    | 0.9260(1)                  | 0.0741(1)              | 0.4351(8)                                   | 5.809(3)                                    | 14.9046                   | 17.939                   | -0.5608                    | 9.481                    |
| 9450                        | 47.182(2)                    | 0.9221(2)                  | 0.0779(2)              | 0.4352(6)                                   | 5.812(2)                                    | 15.2050                   | 18.212                   | -0.2958                    | 9.485                    |
| 9550                        | 47.148(2)                    | 0.9183(2)                  | 0.0816(2)              | 0.4355(3)                                   | 5.805(2)                                    | 15.5024                   | 18.473                   | -0.0142                    | 9.484                    |
| 9575                        | 47.130(2)                    | 0.9179(1)                  | 0.0821(1)              | 0.4355(3)                                   | 5.799(2)                                    | 15.5580                   | 18.515                   | 0.0353                     | 9.482                    |
| 9600                        | 47.134(3)                    | 0.9166(2)                  | 0.0834(2)              | 0.4357(6)                                   | 5.804(2)                                    | 15.6475                   | 18.602                   | 0.1249                     | 9.483                    |
| $P_{\text{imp}} = 52.6$ GPa |                              |                            |                        |   |   |                           |                          |                            |                          |
| 9500                        | 52.740(4)                    | 0.9101(2)                  | 0.0899(2)              | 0.4160(6)                                   | 6.336(3)                                    | 15.7319                   | 19.248                   | -1.9974                    | 9.911                    |
| 9750                        | 52.737(3)                    | 0.9002(2)                  | 0.0998(2)              | 0.4162(4)                                   | 6.325(2)                                    | 16.5027                   | 19.934                   | -1.3053                    | 9.912                    |
| 10 000                      | 52.754(3)                    | 0.8888(2)                  | 0.1112(2)              | 0.4162(4)                                   | 6.314(3)                                    | 17.3362                   | 20.683                   | -0.5620                    | 9.914                    |
| 10 250                      | 52.755(6)                    | 0.8774(2)                  | 0.1226(2)              | 0.4164(8)                                   | 6.304(4)                                    | 18.1791                   | 21.441                   | 0.2006                     | 9.915                    |
| $P_{\text{imp}} = 60.4$ GPa |                              |                            |                        |   |   |                           |                          |                            |                          |
| 10 400                      | 60.527(3)                    | 0.8498(3)                  | 0.1502(3)              | 0.3925(5)                                   | 6.989(2)                                    | 19.4771                   | 23.379                   | -1.7771                    | 10.469                   |
| 10 500                      | 60.521(4)                    | 0.8441(2)                  | 0.1559(2)              | 0.3924(5)                                   | 6.979(2)                                    | 19.8615                   | 23.724                   | -1.4344                    | 10.468                   |
| 10 600                      | 60.563(7)                    | 0.8388(3)                  | 0.1612(3)              | 0.3920(8)                                   | 6.969(4)                                    | 20.2337                   | 24.057                   | -1.1294                    | 10.469                   |
| 10 900                      | 60.551(4)                    | 0.8231(2)                  | 0.1769(2)              | 0.3916(7)                                   | 6.939(2)                                    | 21.3514                   | 25.056                   | -0.1370                    | 10.466                   |
| 10 950                      | 60.506(3)                    | 0.8201(3)                  | 0.1799(3)              | 0.3916(6)                                   | 6.928(4)                                    | 21.5531                   | 25.231                   | 0.0583                     | 10.462                   |
| 11 000                      | 60.544(4)                    | 0.8170(4)                  | 0.1830(4)              | 0.03915(8)                                  | 6.929(2)                                    | 21.7593                   | 25.424                   | 0.2306                     | 10.465                   |
| $P_{\text{imp}} = 81.1$ GPa |                              |                            |                        |   |   |                           |                          |                            |                          |
| 12 400                      | 81.093(5)                    | 0.6487(4)                  | 0.3513(4)              | 0.3352(5)                                   | 8.275(4)                                    | 30.8436                   | 35.438                   | -0.7344                    | 11.728                   |
| 12 500                      | 81.075(7)                    | 0.6416(5)                  | 0.3584(5)              | 0.3347(7)                                   | 8.253(3)                                    | 31.3115                   | 35.854                   | -0.3281                    | 11.724                   |
| 12 600                      | 81.120(8)                    | 0.6351(4)                  | 0.3649(4)              | 0.3343(8)                                   | 8.240(4)                                    | 31.7590                   | 36.259                   | 0.0387                     | 11.724                   |
| $P_{\text{imp}} = 91.5$ GPa |                              |                            |                        |   |   |                           |                          |                            |                          |
| 13 000                      | 91.191(9)                    | 0.5584(6)                  | 0.4416(6)              | 0.3109(7)                                   | 8.775(5)                                    | 35.5438                   | 40.461                   | -1.3754                    | 12.274                   |
| 13 250                      | 91.118(9)                    | 0.5424(5)                  | 0.4576(5)              | 0.3101(8)                                   | 8.725(4)                                    | 35.6715                   | 41.464                   | -0.3756                    | 12.263                   |
| 13 500                      | 91.092(11)                   | 0.5267(7)                  | 0.4733(7)              | 0.3092(8)                                   | 8.671(6)                                    | 37.7904                   | 42.454                   | 0.5857                     | 12.255                   |
| 15 500                      | 90.482(12)                   | 0.4170(6)                  | 0.5830(6)              | 0.3045(11)                                  | 8.242(3)                                    | 46.2912                   | 49.933                   | 8.1337                     | 12.183                   |
| 16 000                      | 90.418(14)                   | 0.3917(6)                  | 0.6083(6)              | 0.3036(12)                                  | 8.147(4)                                    | 48.3805                   | 51.779                   | 9.9691                     | 12.173                   |
| 16 500                      | 90.064(18)                   | 0.3599(8)                  | 0.6401(8)              | 0.3022(17)                                  | 7.991(4)                                    | 50.7644                   | 53.858                   | 12.1530                    | 12.141                   |

<sup>a</sup>Mole fraction of  $N_2$ , so  $x(N_2) = N_{N_2}/N_{\text{total}}$  and  $x(N) = \frac{1}{2}N_N/N_{\text{total}}$ , where  $N_{\text{total}} = 3375$ .<sup>b</sup>From Eq. (11).<sup>c</sup>From Eq. (14).<sup>d</sup>From Eq. (8).<sup>e</sup>From Eq. (7).

TABLE VI. Constant-pressure reactive Monte Carlo simulations of shocked liquid NO.

| $T$<br>(K)                   | $\langle P \rangle$<br>(GPa) | Mole fraction <sup>a</sup>      |                                 |                                | $\langle V \rangle$<br>(cm <sup>3</sup> /g) | $\langle U^{\text{conf}} \rangle$<br>(kJ/g) | $H^{0b}$<br>(kJ/g) | $E^c$<br>(kJ/g) | $H_g^d$<br>(kJ/g) | $D^e$<br>(km/s) |
|------------------------------|------------------------------|---------------------------------|---------------------------------|--------------------------------|---|---|--------------------|-----------------|-------------------|-----------------|
|                              |                              | $\langle x(\text{N}_2) \rangle$ | $\langle x(\text{O}_2) \rangle$ | $\langle x(\text{NO}) \rangle$ |   |   |                    |                 |                   |                 |
| $P_{\text{imp}} = 14.47$ GPa |                              |                                 |                                 |                                |   |   |                    |                 |                   |                 |
| 2250                         | 14.483(1)                    | 0.4791(1)                       | 0.4791(1)                       | 0.0419(1)                      | 0.5077(5)                                   | 1.673(1)                                    | 2.3550             | 3.404           | -1.310            | 5.560           |
| 2500                         | 14.473(2)                    | 0.4649(2)                       | 0.4649(2)                       | 0.0702(2)                      | 0.5123(9)                                   | 1.688(2)                                    | 2.7543             | 3.750           | -0.9286           | 5.604           |
| 2750                         | 14.487(2)                    | 0.4468(2)                       | 0.4468(2)                       | 0.1064(2)                      | 0.5164(9)                                   | 1.705(1)                                    | 3.1788             | 4.122           | -0.5282           | 5.649           |
| 3000                         | 14.476(1)                    | 0.4257(4)                       | 0.4257(4)                       | 0.1486(4)                      | 0.5206(7)                                   | 1.718(1)                                    | 3.6234             | 4.510           | -0.1068           | 5.690           |
| 3250                         | 14.476(2)                    | 0.4026(4)                       | 0.4026(4)                       | 0.1949(4)                      | 0.5241(7)                                   | 1.729(1)                                    | 4.0819             | 4.910           | 0.3198            | 5.728           |
| $P_{\text{imp}} = 17.93$ GPa |                              |                                 |                                 |                                |   |   |                    |                 |                   |                 |
| 2500                         | 17.934(1)                    | 0.4572(2)                       | 0.4572(2)                       | 0.0856(2)                      | 0.4783(6)                                   | 2.042(1)                                    | 2.8008             | 4.150           | -1.323            | 5.909           |
| 2750                         | 17.965(2)                    | 0.4366(2)                       | 0.4366(2)                       | 0.1268(2)                      | 0.4812(9)                                   | 2.061(2)                                    | 3.2400             | 4.539           | -0.9127           | 5.941           |
| 3000                         | 17.921(1)                    | 0.4135(4)                       | 0.4135(4)                       | 0.1730(4)                      | 0.4842(7)                                   | 2.069(2)                                    | 3.6966             | 4.934           | -0.4825           | 5.964           |
| 3250                         | 17.927(2)                    | 0.3885(4)                       | 0.3885(4)                       | 0.2229(4)                      | 0.4866(7)                                   | 2.080(2)                                    | 4.1657             | 5.345           | -0.0506           | 5.988           |
| 3275                         | 17.946(2)                    | 0.3859(6)                       | 0.3859(6)                       | 0.2283(6)                      | 0.4868(7)                                   | 2.083(2)                                    | 4.2133             | 5.389           | -0.0077           | 5.992           |
| 3300                         | 17.944(3)                    | 0.3833(4)                       | 0.3833(4)                       | 0.2333(4)                      | 0.4870(9)                                   | 2.085(2)                                    | 4.2608             | 5.431           | 0.0369            | 5.995           |
| $P_{\text{imp}} = 21.03$ GPa |                              |                                 |                                 |                                |   |   |                    |                 |                   |                 |
| 2700                         | 21.036(2)                    | 0.4314(4)                       | 0.4314(4)                       | 0.1372(4)                      | 0.4565(5)                                   | 2.363(3)                                    | 3.2080             | 4.823           | -1.369            | 6.200           |
| 2900                         | 21.031(1)                    | 0.4119(3)                       | 0.4119(3)                       | 0.1763(3)                      | 0.4580(7)                                   | 2.370(2)                                    | 3.5790             | 5.146           | -1.029            | 6.213           |
| 3100                         | 21.035(2)                    | 0.3911(5)                       | 0.3911(5)                       | 0.2178(5)                      | 0.4596(7)                                   | 2.380(1)                                    | 3.9582             | 5.480           | -0.6785           | 6.229           |
| 3300                         | 21.054(3)                    | 0.3697(5)                       | 0.3697(5)                       | 0.2606(5)                      | 0.4609(9)                                   | 2.391(2)                                    | 4.3422             | 5.819           | -0.3287           | 6.244           |
| 3400                         | 21.061(1)                    | 0.3592(4)                       | 0.3592(4)                       | 0.2815(4)                      | 0.4614(8)                                   | 2.395(2)                                    | 4.5332             | 5.986           | -0.1565           | 6.250           |
| 3500                         | 21.031(2)                    | 0.3489(5)                       | 0.3489(5)                       | 0.3021(5)                      | 0.4623(5)                                   | 2.395(2)                                    | 4.7230             | 6.148           | 0.0207            | 6.254           |
| $P_{\text{imp}} = 25.47$ GPa |                              |                                 |                                 |                                |   |   |                    |                 |                   |                 |
| 3000                         | 25.487(2)                    | 0.3830(8)                       | 0.3830(8)                       | 0.2339(8)                      | 0.4301(14)                                  | 2.800(3)                                    | 3.8790             | 5.848           | -1.430            | 6.584           |
| 3250                         | 25.478(2)                    | 0.3551(9)                       | 0.3551(9)                       | 0.2898(9)                      | 0.4312(8)                                   | 2.809(2)                                    | 4.3654             | 6.274           | -0.9874           | 6.593           |
| 3500                         | 25.508(3)                    | 0.3277(9)                       | 0.3277(9)                       | 0.3445(9)                      | 0.4325(6)                                   | 2.826(2)                                    | 4.8494             | 6.706           | -0.5450           | 6.608           |
| 3750                         | 25.467(2)                    | 0.3024(5)                       | 0.3024(5)                       | 0.3952(5)                      | 0.4336(9)                                   | 2.828(3)                                    | 5.3212             | 7.110           | -0.1177           | 6.613           |
| 4000                         | 25.488(3)                    | 0.2785(8)                       | 0.2785(8)                       | 0.4429(8)                      | 0.4349(7)                                   | 2.843(2)                                    | 5.7857             | 7.520           | 0.3045            | 6.628           |
| $P_{\text{imp}} = 28.47$ GPa |                              |                                 |                                 |                                |   |   |                    |                 |                   |                 |
| 3200                         | 28.455(3)                    | 0.3468(4)                       | 0.3468(4)                       | 0.3065(4)                      | 0.4149(4)                                   | 3.080(2)                                    | 4.3514             | 6.545           | -1.488            | 6.821           |
| 3400                         | 28.477(2)                    | 0.3241(7)                       | 0.3241(7)                       | 0.3518(7)                      | 0.4155(7)                                   | 3.091(2)                                    | 4.7425             | 6.892           | -1.136            | 6.829           |
| 3600                         | 28.475(2)                    | 0.3029(5)                       | 0.3029(5)                       | 0.3943(5)                      | 0.4163(5)                                   | 3.101(2)                                    | 5.1259             | 7.229           | -0.7869           | 6.836           |
| 3800                         | 28.445(4)                    | 0.2831(6)                       | 0.2831(6)                       | 0.4337(6)                      | 0.4172(8)                                   | 3.107(3)                                    | 5.5004             | 7.555           | -0.4434           | 6.840           |
| 4000                         | 28.497(3)                    | 0.2647(8)                       | 0.2647(8)                       | 0.4705(8)                      | 0.4175(7)                                   | 3.116(2)                                    | 5.8672             | 7.875           | -0.1271           | 6.850           |
| 4200                         | 28.492(5)                    | 0.2478(8)                       | 0.2478(8)                       | 0.5044(8)                      | 0.4186(9)                                   | 3.127(3)                                    | 6.2255             | 8.189           | 0.2025            | 6.859           |

<sup>a</sup>Mole fraction of species  $i$ ,  $x(i) = N_i / N_{\text{total}}$ , where  $N$  is the number of particles,  $N_{\text{total}} = 3375$ .

<sup>b</sup>From Eq. (11).

<sup>c</sup>From Eq. (14).

<sup>d</sup>From Eq. (8).

<sup>e</sup>From Eq. (7).

- [1] J. Touret and A. M. van den Kerkhof, *Physica B & C* **139**, 834 (1986).
- [2] P. J. Kortbeek, C. A. T. Seldam, and J. A. Schouten, *Mol. Phys.* **69**, 1001 (1990).
- [3] Z. Duan, N. Moller, and J. H. Weare, *Geochim. Cosmochim. Acta* **60**, 1209 (1996).
- [4] W. Fickett and W. C. Davis, *Detonation* (University of California Press, Berkeley, 1979).
- [5] F. H. Ree, *J. Chem. Phys.* **84**, 5845 (1986).
- [6] L. E. Fried and W. M. Howard, *J. Chem. Phys.* **110**, 12 023 (1999).
- [7] F. H. Ree, J. A. Viecelli, and M. van Thiel, *J. Mol. Liq.* **85**, 229 (2000).
- [8] M. Ross, *J. Chem. Phys.* **71**, 1567 (1979).
- [9] G. Zerah and J. Hansen, *J. Chem. Phys.* **84**, 2336 (1986).
- [10] H. L. Vortler, I. Nezbeda, and M. Lisal, *Mol. Phys.* **92**, 813 (1997).
- [11] L. E. Fried and W. M. Howard, *J. Chem. Phys.* **109**, 7338

- (1998).
- [12] F. H. Ree, *J. Chem. Phys.* **81**, 1251 (1984).
- [13] L. E. Fried, *Cheetah 3.0 User's Manual* (Lawrence Livermore National Laboratory, Livermore, CA, 2001), manuscript number UCRL-MA-117541, Revision 3.
- [14] A. M. Karo, J. R. Hardy, and F. E. Walker, *Acta Astronaut.* **5**, 1041 (1978).
- [15] J. D. Powell and J. H. Batteh, *J. Appl. Phys.* **49**, 3933 (1978).
- [16] J. D. Powell and J. H. Batteh, *Phys. Rev. B* **20**, 1398 (1979).
- [17] J. D. Powell and J. H. Batteh, *J. Appl. Phys.* **51**, 2050 (1980).
- [18] B. L. Holihan, W. G. Hoover, B. Moran, and G. K. Straub, *Phys. Rev. A* **22**, 2798 (1980).
- [19] D. H. Tsai and S. F. Trevino, *J. Chem. Phys.* **81**, 5636 (1984).
- [20] D. H. Tsai, *Chemistry and Physics of Energetic Materials*, edited by S. N. Bulusu (Kluwer, Dordrecht, 1990).
- [21] D. W. Brenner, *Shock Compression of Condensed Matter* (Elsevier, Amsterdam, 1992).
- [22] D. H. Robertson, D. W. Brenner, M. L. Elert, and C. T. White, *Shock Compression of Condensed Matter* (Elsevier, Amsterdam, 1992).
- [23] C. T. White, D. H. Robertson, M. L. Elert, and D. W. Brenner, *Microscopic Simulations of Complex Hydrodynamic Phenomena* (Plenum, New York, 1992).
- [24] J. J. Erpenbeck, *Phys. Rev. A* **46**, 6406 (1992).
- [25] D. W. Brenner, D. H. Robertson, M. L. Elert, and C. T. White, *Phys. Rev. Lett.* **70**, 2174 (1993).
- [26] C. T. White, S. B. Sinnott, J. W. Mintmire, D. W. Brenner, and D. H. Robertson, *Int. J. Quantum Chem., Symp.* **28**, 129 (1994).
- [27] B. M. Rice, W. Mattson, J. Grosh, and S. F. Trevino, *Phys. Rev. E* **53**, 611 (1996).
- [28] B. M. Rice, W. Mattson, J. Grosh, and S. F. Trevino, *Phys. Rev. E* **53**, 623 (1996).
- [29] J.-B. Maillet, M. Mareschal, L. Soulard, R. Ravelo, P. S. Lomdahl, T. C. Germann, and B. L. Holian, *Phys. Rev. E* **63**, 016121 (2000).
- [30] D. R. Swanson, J. W. Mintmire, D. H. Robertson, and C. T. White, *Chem. Phys. Repts.* **18**, 1871 (2000).
- [31] J. D. Kress, S. Mazevet, L. A. Collins, and W. W. Wood, *Phys. Rev. B* **63**, 024203 (2000).
- [32] J. K. Johnson, A. Z. Panagiotopoulos, and K. E. Gubbins, *Mol. Phys.* **81**, 717 (1994).
- [33] W. R. Smith and B. Trřska, *J. Chem. Phys.* **100**, 3019 (1994).
- [34] T. M. Reed and K. E. Gubbins, *Applied Statistical Mechanics* (McGraw-Hill, New York, 1973).
- [35] D. A. McQuarrie, *Statistical Mechanics* (Harper, New York, 1976).
- [36] M. W. Chase, C. A. Davies, J. R. Downey, D. J. Frurip, R. A. McDonald, and A. N. Syverud, *J. Phys. Chem. Ref. Data* **14**, 1530 (1985); **14**, 1533 (1985); **14**, 1551 (1985); **14**, 1667 (1985).
- [37] J. K. Johnson, *Adv. Chem. Phys.* **105**, 461 (1999).
- [38] M. Lřsal and W. R. Smith (private communication).
- [39] M. Lřsal, I. Nezbeda, and W. R. Smith, *J. Chem. Phys.* **110**, 8597 (1999).
- [40] M. Lřsal, W. R. Smith, and I. Nezbeda, *J. Phys. Chem. B* **103**, 10 496 (1999).
- [41] M. Lřsal, W. R. Smith, and I. Nezbeda, *J. Chem. Phys.* **113**, 4885 (2000).
- [42] C. H. Turner, J. K. Johnson, and K. E. Gubbins, *J. Chem. Phys.* **114**, 1851 (2001).
- [43] M. Borówko and R. Zagórski, *J. Chem. Phys.* **114**, 5397 (2001).
- [44] C. H. Turner, J. K. Brennan, J. K. Johnson, and K. E. Gubbins, *J. Chem. Phys.* **116**, 2138 (2002).
- [45] C. H. Turner, J. K. Brennan, J. P. Pikunic, and K. E. Gubbins, *Appl. Surf. Sci.* (to be published).
- [46] N. Metropolis, A. W. Rosenbluth, M. N. Rosenbluth, A. E. Teller, and E. Teller, *J. Chem. Phys.* **21**, 1087 (1953).
- [47] A. Lofthus and P. H. Krupenie, *J. Phys. Chem. Ref. Data* **6**, 113 (1977).
- [48] C. E. Moore and J. W. Gallagher, *Tables of Spectra of Hydrogen, Carbon, Oxygen Atoms and Ions*, CRC Series in Evaluated Data in Atomic Physics (Chemical Rubber, Boca Raton, 1993).
- [49] L. A. Curtiss, P. C. Redfern, and D. J. Furip, *Rev. Comput. Chem.* **15**, 147 (2000).
- [50] J. W. Ochterski, *Thermochemistry in Gaussian* (Gaussian, Carnegie, PA, 2000), <http://www.gaussian.com>
- [51] D. Frenkel and B. Smit, *Understanding Molecular Simulation* (Academic, San Diego, 1996).
- [52] K. P. Huber and G. Herzberg, *Molecular Spectra and Molecular Structure IV, Constants of Diatomic Molecules* (Van Nostrand Reinhold, New York, 1979).
- [53] M. P. Allen and D. J. Tildesley, *Computer Simulation of Liquids* (Oxford University Press, Oxford, 1987).
- [54] V. N. Zubarev and G. S. Telegin, *Sov. Phys. Dokl.* **7**, 34 (1962).
- [55] W. J. Nellis, H. B. Radousky, D. C. Hamilton, A. C. Mitchell, N. C. Holmes, K. B. Christianson, and M. van Thiel, *J. Chem. Phys.* **94**, 2244 (1991).
- [56] H. B. Radousky, W. J. Nellis, M. Ross, D. C. Hamilton, and A. C. Mitchell, *Phys. Rev. Lett.* **57**, 2419 (1986).
- [57] M. Ross, *J. Chem. Phys.* **86**, 7110 (1987).
- [58] A. K. McMahan and R. LeSar, *Phys. Rev. Lett.* **54**, 1929 (1985).
- [59] R. M. Martin and R. J. Needs, *Phys. Rev. B* **34**, 5082 (1986).
- [60] M. van Thiel and F. H. Ree, *J. Chem. Phys.* **104**, 5019 (1986).
- [61] D. C. Hamilton and F. H. Ree, *J. Chem. Phys.* **90**, 4972 (1989).
- [62] M. Ross, *High Press. Res.* **16**, 371 (2000).
- [63] G. L. Schott, M. S. Shaw, and J. D. Johnson, *J. Chem. Phys.* **82**, 4264 (1985).